Indian Journal of Pure & Applied Physics
Vol. 62, June 2024, pp. 441-450
DOI: 10.56042/ijpap.v62i6.8475

# Exploring the Effects of Entrance Channel and Fissility on Pre-scission Neutron Multiplicity and Nuclear Dissipation

Rakesh Kumar[a], Vikas[a], Ranjeet Dalal[b] & Hardev Singh[a*]

[a]Department of Physics, Kurukshetra University, Kurukshetra, Haryana 136 119, India

[b]Centre for Radio Ecology and Department of Physics, Guru Jambheshwar University of Science and Technology, Hisar, Haryana 125 001, India

*Received 1 February 2024; accepted 14 March 2024*

The pre-scission neutron multiplicity and dissipation strength are studied for a systematic understanding of the role of entrance-channel in fusion-fission dynamics using the statistical model formalism. The measured pre-scission neutron multiplicity is found to be higher for symmetric reactions as compared to the asymmetric ones for a given compound nucleus, with the exception of a few reaction channels, where the presence of quasi-fission affects the neutron yield. The calculated pre-scission neutron multiplicities are compared with the experimentally measured values and it is found that for the majority of reactions, the calculated values of pre-scission neutron multiplicities are under-estimated. The under-estimation of pre-scission neutron multiplicity indicates that dissipation is required in the fission channel to reproduce the experimental data. The systematic behaviour of pre-scission neutron multiplicity and dissipation strength as a function of fissility of the compound nucleus is also explored for the select energy ranges. It is found that the pre-scission neutron multiplicity shows nearly increasing behaviour as a function of fissility of the compound nucleus, whereas, dissipation does not seem to follow such an increasing trend for the studied reactions.

**Keywords**: Neutron multiplicity; Entrance channel effect; Dissipation strength; Fissility

## 1 Introduction

Nuclear physics researchers have been exploring the dynamics of heavy ion-induced fusion-fission reactions using both theoretical and experimental methods[1-12]. In a heavy ion-induced fusion-fission reaction, a compound nucleus (CN) is formed that is in equilibrium across all degrees of freedom. The emission of particles like neutron[13-18], gamma[19-20], and charged particles (alpha, proton)[21-22], are the probes which give information about the dynamical evolution of heavy ion induced fusion-fission process. Each of these probes has a unique effect on our understanding of the fusion-fission process. When excitation energy (E*) of the compound system is high enough, neutron emission among these probes becomes the dominating decay mode. The number of neutrons emitted per fission is termed as neutron multiplicity ($M_{pre}$). In a heavy ion induced reaction, neutrons are emitted at distinct stages of CN formation and decay that provides information about the different phases of fusion-fission process[23]. The measurement of pre-scission neutron multiplicity gives information about the dissipation (β) involved in such reactions[24]. Experimental studies have shown that pre-scission neutron multiplicity also plays a crucial role in understanding the phenomenon of quasi-fission (QF)[11,14]. The measurements of $M_{pre}$ and their comparison with the statistical model predictions revealed that measured multiplicities are higher as compared to the values calculated with the statistical model of nuclear fission[23-27]. Dissipative dynamical models are found to be crucial to explain the experimental data because the statistical models, which are based on the transition state method does not include the effect of nuclear dissipation. Several groups have studied the various aspects of neutron multiplicity and nuclear dissipation primarily with a focus on the measurement of the excitation function of pre-scission neutron for a number of reactions[13-18]. In general, it was found that $M_{pre}$ increases with increase in excitation energy of the CN[12-28].

In a recent work, Rai *et al.*[7], studied the effect of entrance channel mass asymmetry (α) by considering the compound nuclei in A~ 200 mass region at nearly matching excitation energy. They found that for the similar values of entrance channel mass asymmetry, and of excitation energy, same amount of dissipation is required to reproduce the experimental data. They also observed that the dissipation decreases with increase in the value of entrance channel mass

*Corresponding author: (E-mail: hsinghphy@kuk.ac.in)

asymmetry. Several other groups also performed the similar type of studies to confirm the effect of entrance channel mass asymmetry on pre-scission neutron multiplicity and dissipation strength[13-16], where the same compound nucleus is populated at the matching excitation energies through different reaction channels. The value of pre-scission neutron multiplicity was found to be higher in the case of relatively symmetric reaction systems as compared to the asymmetric systems[13-15]. The observation of higher $M_{pre}$ for symmetric reactions could be interpreted in terms of the entrance channel mass asymmetry with respect to the Businaro-Gallone mass asymmetry ($\alpha_{BG}$). An asymmetric entrance channel, having $\alpha > \alpha_{BG,}$ leads to a lower yield of average pre-scission neutrons as compared to a symmetric entrance channel, having $\alpha < \alpha_{BG,}$ as the mass flow is from projectile to the target in the former case, thus leading to CN formation on a relatively faster time scale.

Recently, Shareef *et al.*[16], did the statistical model analysis and explored the fission delay time ($t_{delay}$) as a function of fissility of the compound nucleus. They found a systematic increase in $t_{delay}$ with an increase in fissility of the CN. In our recent work, we have explored the statistical model analysis of neutron multiplicity in ~ 200 and 250 mass regions, where dissipation strength was found to be increasing with excitation energy of the CN, in both the mass regions[29]. Despite a considerable amount of data available and the efforts made over the years, a common systematics could not be established for the neutron multiplicity and dissipation strength.

With this motivation, we accessed the data available in literature for the reaction systems with different entrance channel mass asymmetry, forming the same compound nucleus (except for reactions at Sr. No. 27-31 of Table 1, where populated compound

Table 1 — Reaction systems considered for the present analysis along with different entrance channel parameters

| Sr. No. | Reactions | E* | $\alpha$ | $\alpha_{B.G}$ | $\chi$ | $\alpha_{red}$ | $M_{pre}$ (exp.) | $M_{pre}$ ($\beta$=0) | B -fitted | Ref. |
|---|---|---|---|---|---|---|---|---|---|---|
| 1. | $^{28}Si+^{98}Mo\rightarrow^{126}Ba$ | 101.4 | 0.555 | 0.618 | 0.501 | 0.898 | 1.32±0.09 | 0.91 | 3.0 | 25 |
| | | 118.5 | | | | | 2.10±0.13 | 0.79 | 11.5 | |
| | | 131.7 | | | | | 2.52±0.12 | 0.79 | 17.5 | |
| 2. | $^{19}F+^{107}Ag\rightarrow^{126}Ba$ | 101.5 | 0.698 | 0.618 | 0.501 | 1.129 | 1.31±0.17 | 1.08 | 2.0 | 25 |
| | | 118.5 | | | | | 1.85±0.11 | 1.27 | 3.5 | |
| 3. | $^{34}S+^{154}Sm\rightarrow^{188}Pt$ | 66.5 | 0.638 | 0.818 | 0.671 | 0.779 | 2.5±0.07 | 1.47 | 5.7 | 25 |
| | | 100 | | | | | 4.5±0.07 | 1.25 | 28.0 | |
| 4. | $^{19}F+^{169}Tm\rightarrow^{188}Pt$ | 67.64 | 0.798 | 0.818 | 0.671 | 0.975 | 2.51±0.31 | 2.04 | 3.0 | 26 |
| | | 74.8481.13 | | | | | 2.39±0.27 | 2.28 | 0.5 | |
| | | 84.7294.61 | | | | | 2.58±0.25 | 2.44 | 0.8 | |
| | | | | | | | 2.81±0.28 | 2.45 | 1.0 | |
| | | | | | | | 3.31±0.31 | 2.38 | 2.3 | |
| 5. | $^{16}O+^{172}Yb\rightarrow^{188}Pt$ | 99.7 | 0.829 | 0.818 | 0.671 | 1.013 | 5.4±0.6 | 2.54 | 15.8 | 25 |
| 6. | $^{19}F+^{178}Hf\rightarrow^{197}Tl$ | 72.00 | 0.807 | 0.833 | 0.694 | 0.968 | 2.75±0.16 | 2.24 | 1.74 | 13 |
| | | 76.00 | | | | | 3.07±0.13 | 2.28 | 2.60 | |
| | | 81.00 | | | | | 3.57±0.12 | 2.30 | 3.60 | |
| 7. | $^{16}O+^{181}Ta\rightarrow^{197}Tl$ | 72.00 | 0.837 | 0.833 | 0.694 | 1.004 | 2.58±0.13 | 2.37 | 0.5 | 13 |
| | | 76.00 | | | | | 2.79±0.10 | 2.41 | 1.2 | |
| | | 81.00 | | | | | 3.10±0.13 | 2.54 | 1.5 | |
| 8. | $^{28}Si+^{170}Er\rightarrow^{198}Pb$ | 58.11 | 0.717 | 0.840 | 0.705 | 0.853 | 1.61±0.18 | 1.74 | 0.0 | 26 |
| | | 71.08 | | | | | 2.39±0.28 | 1.64 | 2.5 | |
| | | 84.00 | | | | | 3.00±0.37 | 1.56 | 4.5 | |
| 9. | $^{16}O+^{182}W\rightarrow^{198}Pb$ | 45.50 | 0.838 | 0.840 | 0.705 | 0.997 | 1.37±0.53 | 0.93 | 2.1 | 27 |
| | | 53.00 | | | | | 2.41±0.17 | 1.48 | 3.0 | |
| 10. | $^{30}Si+^{170}Er\rightarrow^{200}Pb$ | 75.65 | 0.700 | 0.838 | 0.701 | 0.835 | 2.44±0.30 | 1.44 | 3.2 | 26 |
| 11. | $^{19}F+^{181}Ta\rightarrow^{200}Pb$ | 61.39 | 0.810 | 0.838 | 0.701 | 0.966 | 1.87±0.19 | 1.99 | 0.0 | 26 |
| | | 70.46 | | | | | 2.65±0.17 | 2.30 | 1.1 | |
| | | 79.48 | | | | | 2.72±0.17 | 2.40 | 1.1 | |
| | | 88.54 | | | | | 3.35±0.30 | 2.40 | 2.0 | |
| | | 97.59 | | | | | 3.72±0.36 | 2.32 | 2.7 | |

(*contd.*)

Table 1 — Reaction systems considered for the present analysis along with different entrance channel parameters (*contd.*)

| Sr. No. | Reactions | E* | $\alpha$ | $\alpha_{B.G}$ | $\chi$ | $\alpha_{red}$ | $M_{pre}$ (exp.) | $M_{pre}$ ($\beta$=0) | B -fitted | Ref. |
|---|---|---|---|---|---|---|---|---|---|---|
| 12. | $^{28}Si+^{176}Yb\rightarrow^{204}Po$ | 86 | 0.725 | 0.848 | 0.720 | 0.855 | 3.40 ±00 | 1.51 | 8.0 | 28 |
| | | 106 | | | | | 4.50±00 | 1.50 | 16.6 | |
| 13. | $^{24}Mg+^{180}Hf\rightarrow^{204}Po$ | 95 | 0.765 | 0.848 | 0.720 | 0.902 | 3.90±00 | 1.64 | 8.0 | 28 |
| | | 110 | | | | | 4.80±00 | 1.62 | 14.3 | |
| 14. | $^{20}Ne+^{186}W\rightarrow^{206}Po$ | 96 | 0.806 | 0.847 | 0.717 | 0.951 | 4.0±00 | 2.30 | 4.1 | 28 |
| | | 125 | | | | | 5.0±00 | 2.26 | 7.1 | |
| 15. | $^{16}O+^{190}Os\rightarrow^{206}Po$ | 91.0 | 0.845 | 0.847 | 0.717 | 0.997 | 3.60±00 | 2.43 | 2.4 | 28 |
| | | 129 | | | | | 5.90±00 | 2.46 | 6.0 | |
| 16. | $^{12}C+^{194}Pt\rightarrow^{206}Po$ | 76.6 | 0.883 | 0.847 | 0.717 | 1.042 | 2.8±00 | 2.78 | 0.0 | 28 |
| | | 120 | | | | | 5.4±00 | 2.86 | 4.0 | |
| 17. | $^{12}C+^{194}Pt\rightarrow^{206}Po$ | 49.3 | 0.883 | 0.847 | 0.717 | 1.042 | 1.30±0.13 | 1.66 | 0.0 | 36 |
| | | 54.3 | | | | | 1.59±0.16 | 2.22 | 0.0 | |
| | | 59.4 | | | | | 2.61±0.24 | 2.44 | 0.0 | |
| 18. | $^{18}O+^{192}Os\rightarrow^{210}Po$ | 65.20 | 0.828 | 0.844 | 0.712 | 0.981 | 2.15±0.23 | 2.46 | 0.0 | 26 |
| | | 73.00 | | | | | 2.74±0.22 | 2.85 | 0.0 | |
| | | 88.00 | | | | | 3.65±0.34 | 2.80 | 2.0 | |
| | | 91.74 | | | | | 3.86±0.37 | 2.81 | 2.3 | |
| 19. | $^{12}C+^{198}Pt\rightarrow^{210}Po$ | 49.30 | 0.886 | 0.844 | 0.712 | 1.049 | 1.11±0.10 | 1.50 | 0.0 | 36 |
| | | 54.30 | | | | | 1.31±0.13 | 1.83 | 0.0 | |
| | | 62.20 | | | | | 2.10±0.19 | 2.30 | 0.0 | |
| 20. | $^{19}F+^{194}Pt\rightarrow^{213}Fr$ | 49.80 | 0.821 | 0.861 | 0.743 | 0.953 | 1.91±0.10 | 2.22 | 0.0 | 23 |
| | | 55.30 | | | | | 2.13±0.10 | 2.07 | 0.0 | |
| | | 62.00 | | | | | 2.63±0.10 | 2.01 | 1.5 | |
| | | 67.50 | | | | | 2.87±0.20 | 1.99 | 2.5 | |
| | | 74.00 | | | | | 3.37±0.19 | 1.95 | 3.7 | |
| | | 80.00 | | | | | 3.90±0.21 | 1.90 | 5.6 | |
| | | 86.00 | | | | | 4.45±0.20 | 1.91 | 7.3 | |
| | | 91.80 | | | | | 4.71±0.19 | 1.95 | 8.1 | |
| 21. | $^{16}O+^{197}Au\rightarrow^{213}Fr$ | 52.76 | 0.850 | 0.861 | 0.743 | 0.987 | 2.64±0.23 | 1.99 | 2.3 | 26 |
| | | 62.93 | | | | | 2.67±0.23 | 1.95 | 2.1 | |
| | | 72.18 | | | | | 3.28±0.20 | 1.98 | 3.6 | |
| | | 80.50 | | | | | 3.27±0.32 | 1.95 | 2.9 | |
| 22. | $^{30}Si+^{186}W\rightarrow^{216}Ra$ | 49.5 | 0.722 | 0.865 | 0.751 | 0.834 | 1.96±0.11 | 2.03 | 0.0 | 37 |
| | | 54.6 | | | | | 2.17±0.12 | 1.91 | 1.1 | |
| | | 60.70 | | | | | 2.31±0.13 | 1.76 | 1.7 | |
| | | 66.7 | | | | | 2.66±0.14 | 1.71 | 2.8 | |
| | | 72.8 | | | | | 2.85±0.15 | 1.69 | 3.5 | |
| | | 78.8 | | | | | 3.28±0.15 | 1.66 | 4.5 | |
| | | 84.0 | | | | | 3.36±0.17 | 1.67 | 5.2 | |
| | | 90.0 | | | | | 4.17±0.19 | 1.69 | 8.4 | |
| 23. | $^{19}F+^{197}Au\rightarrow^{216}Ra$ | 53.50 | 0.824 | 0.865 | 0.751 | 0.952 | 1.97±0.13 | 2.44 | 0.0 | 14 |
| | | 57.10 | | | | | 2.42±0.12 | 2.50 | 0.0 | |
| | | 60.80 | | | | | 2.71±0.12 | 2.34 | 1.0 | |
| | | 64.40 | | | | | 2.99±0.10 | 2.31 | 2.0 | |
| | | 71.70 | | | | | 3.52±0.11 | 2.23 | 3.0 | |
| 24. | $^{12}C+^{204}Pb\rightarrow^{216}Ra$ | 42.40 | 0.888 | 0.865 | 0.751 | 1.026 | 1.09±0.19 | 2.15 | 0.0 | 14 |
| | | 46.20 | | | | | 1.27±0.16 | 2.27 | 0.0 | |
| | | 50.00 | | | | | 1.49±0.15 | 2.31 | 0.0 | |
| | | 53.80 | | | | | 1.80±0.10 | 2.30 | 0.0 | |
| | | 57.50 | | | | | 2.05±0.12 | 2.32 | 0.0 | |
| | | 61.30 | | | | | 2.31±0.11 | 2.33 | 0.0 | |

(*contd.*)

Table 1 — Reaction systems considered for the present analysis along with different entrance channel parameters (*contd.*)

| Sr. No. | Reactions | E* | $\alpha$ | $\alpha_{B.G}$ | $\chi$ | $\alpha_{red}$ | $M_{pre}$ (exp.) | $M_{pre}$ ($\beta$=0) | B -fitted | Ref. |
|---|---|---|---|---|---|---|---|---|---|---|
| 25. | $^{40}Ar+^{180}Hf\rightarrow^{220}Th$ | 47.78 | 0.636 | 0.874 | 0.770 | 0.727 | 1.7±0.30 | 0.89 | 2.6 | 38 |
| | | 55.95 | | | | | 1.8±0.30 | 0.89 | 3.0 | |
| | | 77.23 | | | | | 2.3±0.40 | 0.96 | 4.7 | |
| | | 104 | | | | | 3.6±0.40 | 1.23 | 6.5 | |
| 26. | $^{16}O+^{204}Pb\rightarrow^{220}Th$ | 40 | 0.854 | 0.874 | 0.770 | 0.977 | 2.21±0.10 | 1.16 | 2.9 | 39 |
| | | 46.67 | | | | | 2.61±0.10 | 1.26 | 3.7 | |
| | | 58.03 | | | | | 3.81±0.10 | 1.38 | 13.5 | |
| | | 64 | | | | | 4.34±0.06 | 1.46 | 19.0 | |
| 27. | $^{30}Si+^{197}Au\rightarrow^{227}Np$ | 44.10 | 0.736 | 0.885 | 0.796 | 0.831 | 2.03±0.16 | 0.32 | 12.0 | 40 |
| | | 50.20 | | | | | 2.17±0.13 | 0.37 | 13.5 | |
| | | 56.20 | | | | | 2.49±0.15 | 0.44 | 13.7 | |
| | | 62.20 | | | | | 2.80±0.15 | 0.50 | 14.0 | |
| | | 67.50 | | | | | 3.00±0.18 | 0.57 | 14.3 | |
| | | 73.60 | | | | | 3.40±0.27 | 0.64 | 16.0 | |
| | | 78.80 | | | | | 3.64±0.22 | 0.71 | 16.0 | |
| 28. | $^{20}Ne+^{209}Bi\rightarrow^{229}Np$ | 75.99136.00 | 0.825 | 0.884 | 0.793 | 0.933 | 3.20±0.40 | 0.99 | 5.5 | 41 |
| | | | | | | | 5.12±0.40 | 1.99 | 6.3 | |
| 29. | $^{16}O+^{232}Th\rightarrow^{248}Cf$ | 49.50 | 0.871 | 0.897 | 0.826 | 0.971 | 1.35±0.16 | 0.72 | 2.0 | 6 |
| | | 55.20 | | | | | 1.82±0.16 | 0.85 | 3.0 | |
| | | 60.80 | | | | | 2.53±0.18 | 0.97 | 4.8 | |
| 30. | $^{11}B+^{232}Np\rightarrow^{243}Cf$ | 54.10 | 0.909 | 0.899 | 0.833 | 1.011 | 1.35±0.14 | 0.53 | 3.0 | 6 |
| | | 59.90 | | | | | 1.85±0.16 | 0.65 | 4.0 | |
| 31. | $^{48}Ti+^{160}Gd\rightarrow^{208}Rn$ | 56.0 | 0.538 | 0.859 | 0.739 | 0.626 | 2.37±0.08 | 0.83 | 22 | 42 |
| | | 61.4 | | | | | 2.69±0.07 | 0.48 | 36 | |
| | | 66.1 | | | | | 2.78±0.06 | 0.50 | 38 | |
| | | 70.7 | | | | | 2.97±0.06 | 0.54 | 42 | |
| | | 76.2 | | | | | 3.33±0.07 | 0.56 | 48 | |
| | | 80.8 | | | | | 3.45±0.07 | 0.60 | 50 | |
| 32. | $^{30}Si+^{178}Hf\rightarrow^{208}Rn$ | 54.50 | 0.711 | 0.859 | 0.739 | 0.827 | 2.76±0.07 | 1.27 | 18 | 42 |
| | | 59.60 | | | | | 3.08±0.07 | 1.31 | 26 | |
| | | 64.80 | | | | | 3.22±0.07 | 1.08 | 27 | |
| | | 69.10 | | | | | 3.58±0.07 | 1.03 | 37 | |
| | | 74.20 | | | | | 3.80±0.08 | 1.03 | 45 | |
| | | 79.40 | | | | | 3.94±0.08 | 1.03 | 47 | |

nuclei are different isotopes of Np and Cf) at nearly or exactly matching excitation energies in order to explore the effect of entrance channel on pre-scission neutron multiplicity and dissipation strength. Although, the dissipation strength has been previously calculated for some of the chosen reactions either using different models or different versions of the same model, but for the sake of uniformity and to have a reasonable comparison on the same footing, we have calculated the dissipation strength values for all the mentioned reactions using the statistical model code VECSTAT[10].

Further, we have attempted to explore the $M_{pre}$ and dissipation strength as a function of fissility of the CN. In order to study the systematic behavior of pre-scission neutron multiplicity and dissipation strength as a function of fissility ($\chi$) of the compound nucleus, excitation energies for the considered reactions are grouped into three different bins, $E^*_1 = (50 < E^*_1 \leq 60)$ MeV, $E^*_2 = (60 < E^*_2 \leq 70)$ MeV, and $E^*_3 = (70 < E^*_3 \leq 80)$ MeV. For certain reactions, there are multiple data points within a given energy bin and we have considered the data point corresponding to the highest excitation energy in that bin.

## 2 Theoretical Analysis

### 2.1 Model calculations using Bohr-Wheeler fission width

In order to compare the experimental and calculated values of pre-scission neutron multiplicity, we performed the statistical model calculations using the code VECSTAT [10]. This model considers the emission of light charged particles, neutrons, GDR $\gamma$-rays, and fission of the compound nucleus as possible decay channels. The decay widths of the light

particles and GDR γ-rays were obtained from the Weisskopf formula[30]. Initially, we performed the model calculations using the Bohr-Wheeler fission width[31] which is defined as,

$$\Gamma_{BW} = \frac{1}{2\pi\rho_g(E_i)}\int_0^{E_i-V_B}\rho_s\,(E_i - V_B - \varepsilon)d\varepsilon, \quad \text{... (1)}$$

where, $E_i$ is the energy of the initial state, $\rho_g$ and $\rho_s$ are defined as the level densities at ground and saddle configurations, respectively, and $V_B$ is the spin dependent fission barrier given as,

$$V_B = B_f^{FRLDM}(l) - (\delta_g - \delta_s), \quad \text{... (2)}$$

where, $B_f^{FRLDM}(l)$ is the angular momentum dependent FRLDM fission barrier[32]. $\delta_g$ and $\delta_s$ are the shell correction energies for ground-state and saddle configurations, respectively[33]. The level density parameter used is given by[34],

$$a(E^*) = \tilde{a}\left(1 + \frac{f(E^*)}{E^*}\delta M\right), \quad \text{... (3)}$$

with

$$f(E^*) = 1 - e^{-E^*/E_D}. \quad \text{.... (4)}$$

The variable, $\tilde{a}$ is the asymptotic level density and $E_D$ is a parameter that decides the rate at which the shell effects disappear with an increase in the intrinsic excitation energy[35] and δM is the shell correction taken from the difference between the experimental and liquid drop model masses as,

$$\delta M = M_{experimental} - M_{LDM}. \quad \text{... (5)}$$

For simplicity, wherever possible we have arranged the tabular data in accordance to the reduced entrance channel mass asymmetry ($\alpha_{red}$) for compound nucleus, which is defined as the ratio of the entrance channel mass asymmetry (α) to Businaro-Gallone mass asymmetry ($\alpha_{BG}$). The value of $\alpha_{red}$ determine the direction of mass flow between the projectile and target nucleus. The asymmetric reaction systems have larger value of $\alpha_{red}$ as compared to symmetric one, which indicate that the mass flow will be from projectile to target for asymmetric reaction channels and vice versa for symmetric reactions. In equational form, the reduced entrance channel mass asymmetry is given as,

$$\alpha_{red} = \alpha/\alpha_{BG}, \quad \text{.... (6)}$$

where, α is the entrance channel mass asymmetry which is calculated as,

$$\alpha = (A_T - A_P)\,/\,(A_T + A_P), \quad \text{... (7)}$$

where, $A_P$ and $A_T$ are the masses of the projectile and target nuclei, respectively, and $\alpha_{BG}$ is calculated using the empirical relation given by Abe *et al.*[4],

$$\alpha_{BG} = \begin{cases} 0, & \chi < \chi_{BG}, \\ p\sqrt{\frac{(\chi - \chi_{BG})}{(\chi - \chi_{BG}) + q}}, & \chi > \chi_{BG}, \end{cases} \quad \text{... (8)}$$

where $\chi_{BG}$ = 0.396 is the fissility at Businaro-Gallone point, p = 1.12, and q = 0.24. χ is the fissility of compound nucleus and is calculated as,

$$\chi = \frac{Z^2/A}{50.883[1 - 1.7826(N-Z)/A^2]}, \quad \text{... (9)}$$

where, A and Z represent the mass number and atomic number of the compound nucleus, respectively.

The details of the reactions considered for analysis and their relevant parameters are given in Table 1.

The measured pre-scission neutron multiplicities along with statistical model calculations, using Bohr-Wheeler fission width without incorporation of any dissipation in fission channel (β = 0), for few selected compound nuclei covering the entire mass range of populated compound nuclei chosen for the present study (cf. Table 1.) as a function of excitation energy are shown in Fig. 1.

From Fig. 1, it is observed that the measured pre-scission neutron multiplicities increase with excitation energy of the compound nucleus, whereas calculated values show either no dependence or very negligible increase with excitation energy. Both, the experimental and theoretical trends are observed to be same starting from relatively lighter compound nucleus ($^{126}$Ba) to very heavy compound nucleus ($^{248}$Cf), spanning the entire data set as given in Table 1. It is also evident that the measured pre-scission neutron multiplicity is higher for symmetric systems as compared to asymmetric systems except for reaction channels forming the compound nucleus $^{208}$Rn. For $^{208}$Rn, CN formed via $^{30}$Si+$^{178}$Hf has higher values of pre-scission neutron multiplicity as compared to that of $^{48}$Ti+$^{160}$Gd, as $^{30}$Si induced reaction spend significant amount of time during the fusion process before attaining the complete equilibration whereas, in $^{48}$Ti induced reaction, the fast quasi-fission plays a key role in the dynamics of the reaction. Since quasi-fission occurs on a faster time scale as compared to fusion-fission, a smaller

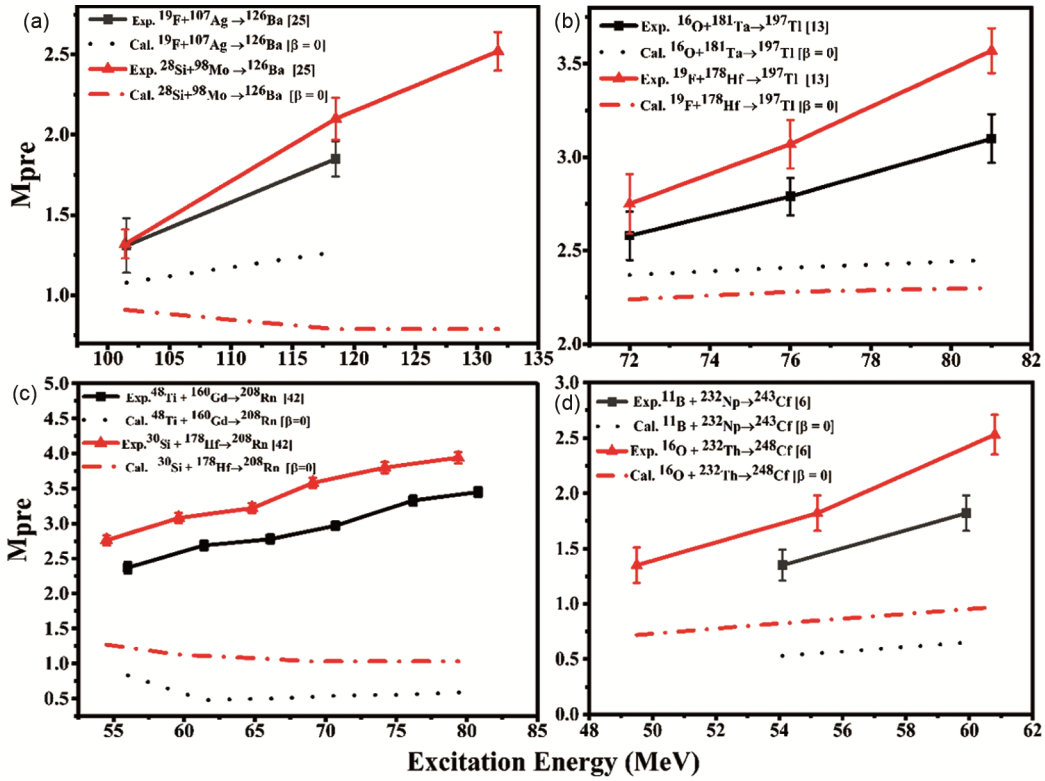


Fig. 1 — Experimental pre-scission neutron multiplicities along with model calculations (β = 0) as a function of excitation energy of the compound nucleus

number of average neutrons are expected to be emitted in quasi-fission. Similar type of behaviour can also be seen in case of the reactions, $^{40}$Ar+$^{180}$Hf→$^{220}$Th and $^{16}$O+$^{204}$Pb→$^{220}$Th. Since experimental yield increases with E* and calculated values do not show any dependence on E*, the difference between measured and calculated neutron multiplicities increases with the excitation energy of the compound nucleus. The comparison suggests that the calculated values are highly underestimated when obtained without incorporation of dissipation in fission channel, and underestimation further increases with increase in excitation energy. The underestimation of pre-scission neutron multiplicity suggests that there might not be enough time for these particles to evaporate before fission. In order to account for this disparity, the excess yield of experimental pre-scission neutron multiplicities was analysed after incorporating the nuclear dissipation in fission channel.

### 2.2 Model Calculations using Kramers fission width

In order to reproduce the experimental pre-scission neutron multiplicities, we performed the statistical model calculations using the Kramers fission width[43] as,

$$\Gamma_K = \frac{\hbar\omega_g}{2\pi} exp(-\frac{V_B}{T}) \left\{ \sqrt{1 + (\frac{\beta}{2\omega_s})^2} - \frac{\beta}{2\omega_s} \right\}, \quad \ldots (10)$$

where β ($10^{21}$ $s^{-1}$) is the dissipation coefficient, treated as a free parameter in the calculations, $\omega_g$ and $\omega_s$ are the frequencies of the harmonic oscillator at the ground state and saddle configurations, respectively. The best fit values of dissipation strength required to reproduce the experimental data for all the chosen reactions in the present study are given in Table 1 and dissipation strength values for the selected reactions that are used in Fig. 1, are shown in Fig. 2.

Figure 2 shows that the dissipation strength also increases with an increase in excitation energy, which is consistent with the observed trend in experimental data. With an increase in excitation energy, neutron emission probability is also expected to increase. Moreover, additional deformation space becomes available to the excited nucleus, which, due to viscosity effects, could take longer to fission. Consequently, higher values of experimental pre-scission neutron multiplicity as well as dissipation strength at higher excitation energies, may primarily be attributed to the contributions arising from the

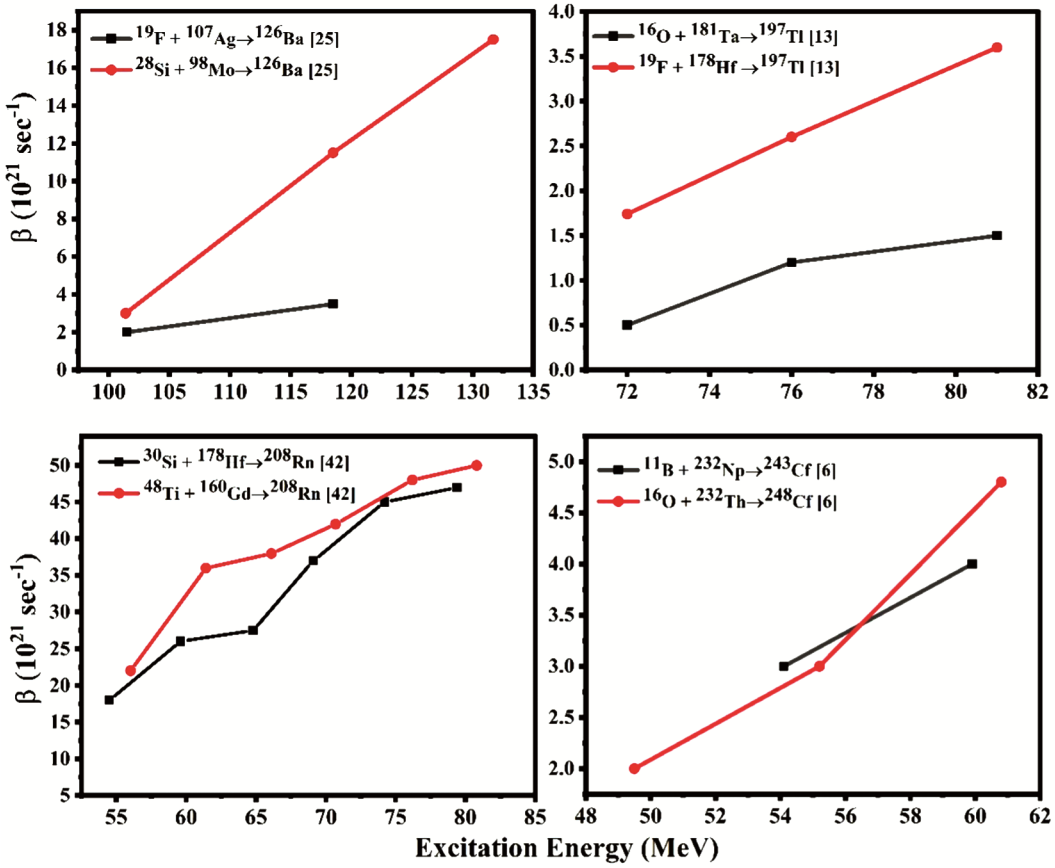


Fig. 2 — Dissipation strength as a function of excitation energy of the compound nucleus

reasons aforementioned. It is also anticipated that two distinct entrance channels populating same compound nucleus will have different formation times. Therefore, the number of neutrons emitted during formation time would be different. As a result, the dissipation strength obtained for different entrance channels is expected to be different due to difference in formation time. The difference in dissipation strength values for different entrance channels of a given CN, required to fit the experimental data, increases with increase in excitation energy of the compound nucleus indicating larger formation time for symmetric reactions as compared to asymmetric ones. The dissipation strength increases at a faster pace for symmetric reactions as compared to the asymmetric reactions. This further reflects that the formation time is larger for symmetric reactions compared to asymmetric reactions.

## 3 Systematics of pre-scission neutron multiplicity and dissipation strength

The fissility of a compound nucleus, which signifies its likelihood to undergo fission, plays a crucial role in influencing the emission of pre-scission neutrons and the dissipation strength in nuclear fission process. In heavy ion-induced reactions, different compound nuclei, populated at same excitation energy, with varying fissility may give distinct pre-scission neutron multiplicity patterns. In the extensive literature, exploring the effect of fissility on pre-scission neutron multiplicity and dissipation, a consensus emerges regarding the intricate relationship between these parameters in nuclear fission. Many studies have highlighted that fissility significantly influences the pre-scission neutron emission and dissipation involved in these reactions. It is also revealed that as the fissility of the compound nucleus increases, the saddle -to-scission time is expected to increase[6]. Consequently, the neutrons emitted during the transition from the saddle to scission constitute an extra count of pre-scission neutrons. Thus, it is expected that pre-scission neutron multiplicity shows an increasing trend with the fissility of the compound nucleus. Moreover, highly fissile compound nuclei often have more deformable shapes, allowing them to access a broader range of nuclear configurations. The

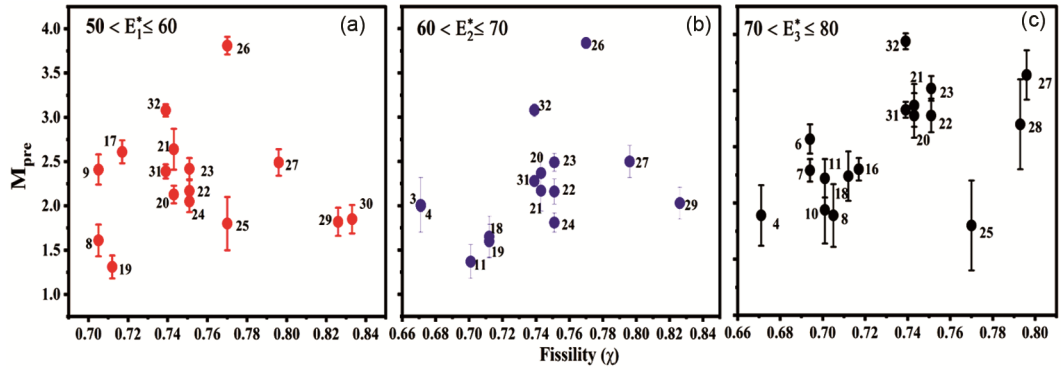


Fig. 3 — Pre-scission neutron multiplicity as a function of fissility of the CN. Numerical value of symbol denotes the serial No. of the reaction in the Table

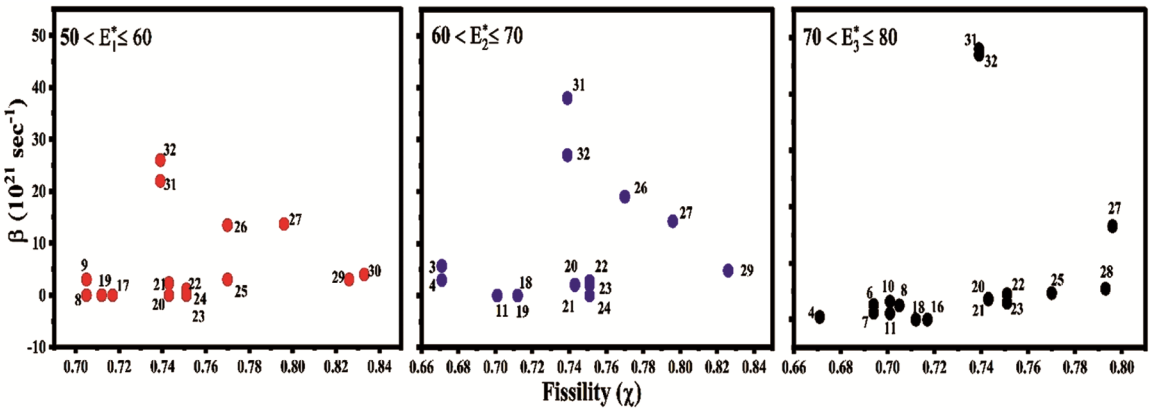


Fig. 4 — Dissipation strength as a function of fissility of the CN. Numerical value of symbol denotes the serial No. of the reactions in the Table

increased deformability impacts the potential energy landscape, affecting the energy distribution within the nucleus. This influences the fission process, neutron emission, and subsequent dissipation strength. In order to study the behavior of $M_{pre}$ as a function of fissility of the compound nucleus, we selected a set of reactions in different energy bins, as shown in Fig. 3.

From Fig. 3, it is evident that the measured pre-scission neutron multiplicities follow the expected trend of nearly increasing behavior with increase in the fissility of the CN for all the selected energy bins. However, this increasing trend is less pronounced and more scattered for the lowest energy bin ($E^*_1$). For more than one data points at a given fissility, the measured $M_{pre}$ is consistently higher for symmetric systems compared to asymmetric systems, except for reaction channels forming the compound nuclei $^{208}$Rn and $^{220}$Th. The dissipation required to reproduce the $M_{pre}$ data presented in Fig. 3, is shown in Fig. 4.

From Fig. 4, it becomes evident that when plotted as a function of fissility, the dissipation strength values have a rather poor resemblance to the increasing trend as observed for experimental data. The variation seems to be almost independent of fissility across the entire fissility range, for all excitation energy bins. However, variation of dissipation for the fission of relatively heavier compound nuclei ($^{220}$Th, $^{227}$Np, $^{208}$Rn) exhibits high β values and it deviates from the general trend of being independent of fissility of the CN. This deviation is particularly prominent in the fission of $^{208}$Rn. For majority of selected reactions, it varies between the dissipation strength value of 0-10. For multiple data points at the same fissility, data from symmetric reactions have higher values of dissipation strength compared to the one corresponding to asymmetric reactions. These results suggest that fusion process for symmetric and asymmetric systems is distinct, as the fusion mechanism, among other factors, also depends on the entrance channel mass asymmetry relative to the critical Businaro-Gallone mass asymmetry.

## 4 Summary and Conclusion

Statistical model calculations were performed for a comprehensive set of reactions, to investigate the effect of entrance channels on both pre-scission neutron multiplicity and dissipation strength. The pre-scission neutron multiplicity and dissipation strength are also explored as a function of fissility of the CN. The measured pre-scission neutron multiplicity was found to be higher for symmetric reaction systems compared to asymmetric reaction systems, except for reaction channels forming the compound nuclei $^{208}$Rn and $^{220}$Th. The comparison between measured and calculated values shows that the calculated values of pre-scission neutron multiplicity are underestimated for majority of reactions. The measured pre-scission neutron multiplicity follows an increasing trend as a function of fissility of the compound nucleus, with the exception of lowest energy bin, where dependence of $M_{pre}$ is rather scattered. The dissipation strength as a function of fissility does not seem to follow any specific dependence for all three energy bins.

## References


1 Lestone J P, Leigh J R, Newton J O, Hinde D J, Wei J X, Chen J X, Elfstrom S & Popescu D G, *Phys Rev C*, 67 (1991) 1078.

2 Hinde D J, Charity R J, Foote G S, Leigh J R, Newton J O, Ogaza S & Chatterjee A, *Nucl Phys A*, 452 (1986) 550.

3 Rossner H, Hilscher D, Hinde D J, Gebauer B, Lehmann M, Wilpert M & Mordhorst E, *Phys Rev C*, 40 (1989) 2629.

4 Abe M, KEK Reports 86-26, KEK TH-28 (1986).

5 Back B B, Blumenthal D J, Davids C N, Henderson D J, Hermann R, Hofman D J, Jiang C L, Penttila H T & Wuosmaa A H, *Phys Rev C*, 60 (1999) 044602.

6 Saxena A, Chatterjee A, Choudhury R K, Kapoor S S & Nadkarni D M, *Phys Rev C*, 49 (1994) 932.

7 Rai N K, Gandhi A, Kumar A, Saneesh N, Kumar M, Kaur G, Parihari A, Arora D, Golda K S, Jhingan A, Sugathan P, Gaush T K, Sadhukhan J, Nayak B K, Deb N K, Biswas S & Chakaraborty A, *Phys Rev C*, 100 (2019) 014614.

8 Vikas & Singh H, *Eur Phys J Plus*, 138 (2023) 695.

9 Vikas, Kavita, Golda K S, T Ghosh K, Jhingan A, P Sugathan, Chatterjee A, Behera B R, Kumar A, Kumar R, Saneesh N, Kumar M, Yadav A, Yadav C, Kumar N, Banerjee A, Rani A, Duggi S K, Dubey R, Rani K, Noor S, Kajal, Acharya J & Singh H, *J Phys G: Nucl Part Phys*, 51 (2024) 035103.

10 Jhilam S & Pal S, *Phys Rev C*, 78 (2008) 011603(R).

11 Hinde D J, Hilscher D, Rossner H, Gebauer B, Lehmann M & Wilpert M, *Phys Rev C*, 45 (1992) 1229.

12 Ramamurthy V S, Kapoor S S, Choudhury R K, Saxena A, Nadkarni D M, Mohanty A K, Nayak B K, Sastry S V, Kailas S, Chatterjee A, Singh P & Navin A, *Phys Rev Lett*, 65 (1990) 25.

13 Singh H, Kumar A, Behera B R & Govil I M, Golda K S, Kumar P, Jhingan A, Singh R P, Sugathan P, Chatterjee M B & Datta S K, Ranjeet, Pal S & Viesti G, *Phys Rev C*, 76 (2007) 044610.

14 Singh H, Golda K S, Pal S, Ranjeet, Sandal R, Behera B R, Singh G, Jhingan A, Singh R P, Sugathan P, Chatterjee M B, Datta S K, Kumar Ajay, Viesti G & Govil I M, *Phys Rev*, 78 (2008) 024609.

15 Singh Hardev, Behera B R, Singh G & Govil I M, Golda K S, Jhingan A, Singh R P, Sugathan P, Chatterjee M B & Datta S K, Pal S, Ranjeet & Mandal S, Shidling P D & Viesti G, *Phys Rev C*, 80 (2009) 064615.

16 Shareef M, Chatterjee A & Prasad E, *Eur Phys J*, 52 (2016) 342.

17 Banerjee T, Nath S & Pal S, *Phys Rev C*, 99 (2019) 024610.

18 Sandal R, Behera B R, Singh V, Kaur M, Kumar A, Singh G, Singh K P, Sugathan P, Jhingan A, Golda K S, Chatterjee M B, Bhowmik R K, Kalkal S, Siwal D, Goyal S, Mandal S, Prasad E, Mahata K, Saxena A, Sadhukhan J & Pal S, *Phys Rev C*, 87 (2013) 014604.

19 Dioszegi I, Shaw N P, Mazumdar I, Hatzikoutelis A & Paul P, *Phys Rev C*, 61 (2000). 024613.

20 Dioszegi I, Shaw N P, Bracco A, Camera F, Tettoni S, Mattiuzzi M & Paul P, *Phys Rev C*, 63 (2000) 014611.

21 Ramachandran K, Chatterjee A, Navin A, Mahata K, Shrivastava A, Tripathi V, Kailas S, Nanal V, Pillay R G, Saxena A, Thomas R G, Kumar S & Sahu P K, *Phys Rev C*, 73 (2006) 064609.

22 Cabrera J, Keutgen Th, Masri Y El, Dufauquez C, Roberfroid V, Tilquin I, Mol J V, Régimbart R, Charity R J, Natowitz J B, Hagel K, Wada R & Hinde D J, *Phys Rev C*, 68 (2003) 034613.

23 Singh V, Behera B R, Kaur Maninder, Sugathan P, Golda K S, Jhingan A, Sadhukhan J, Siwal D, Goyal S, Santra S, Kumar A, Bhowmik R K, Chatterjee M B, Saxena A, Pal S & Kailas S, *Phys Rev C*, 87 (2013) 064601.

24 Mahajan R, Behera B R, Thakur M, Kaur G, Sharma P, Kapoor K, Kumar A, Sugathan P, Jhingan A, A Chatterjee, Saneesh N, Yadav A, Dubey R, Kumar N, Singh H, Saxena A & Santanu Pal, *Phys Rev C*, 98 (2018) 034601.

25 Pomorski K, Nerlo-Pomorska B, Surowiec A, Kowal M, Bartel J, Dietrich K, Richert J, Schmitt C, Benoit B, Brennand E de G, Donadille L & Badimon C, *Nucl Phys A*, 679 (2000) 25.

26 Newton J O, Hinde D J, Charity R J, Leigh J R, Bokhrst J J M, Chatterjee A, Foote G S & Ogaza S, *Nucl Phys A*, 483 (1988) 126.

27 Mahata K, Kailas S & Kapoor S S, *Phys Rev C*, 74 (2006) 041301(R).

28 Chubaryan G G, Itkis M G, Lukyanov S M, Okolovich V N, Penionzhkevic Y E, Rusanov A Y, Salamatin V S & Smirenkin G N, *Phys At Nucl*, 56 (1993) 286.

29 Kumar R, Vikas & Singh H, *Indian J Pure Appl Phys*, 61 (2023) 923.

30 Frobrich P & Gontchar I I, *Phys Rep*, 292 (1998) 131.

31 Bohr N & Wheeler J A, *Phys Rev*, 56 (1939) 426.

32 Sierk A J, *Phys Rev C*, 33 (1986) 2039.

33 Myers W D & Swiatecki W J, *Nucl Phys*, 81 (1966) 1.

34 Ignatyuk A, Smirenkin G & Tishin A, *Yad Fiz*, 21 (1975) 485.

35 Reisdorf W, *Z Phys A*, 300 (1981) 227.
36 Golda K S, Saxena A, Mittal V K, Mahata K, Sugathan P, Jhingan A, Singh V, Sandal R, Goyal S, Gehlot J, Dhal A, Behera B R, Bhowmik R K & Kailas S, *Nucl Phys A*, 913 (2013) 157.
37 Shareef M, Prasad E, Jhingan A, Saneesh N, Pal Santanu, Kumar A M V, Golda K S, Kumar M, Shamlath A, Laveen P V, Visakh A C, Hosamani M M, Duggi S K, Devi P S, Jyothi G N, Tejaswi A, Chatterjee A & Sugathan P, *Phys Rev C*, 107 (2023) 054619.
38 Rubchenya V A, Kuznetsov A V, W Trzaska H, Vakhtin D N, Alexandrov A A, Alkhazov I D, Aysto J, Khlebnikov S V, Lyapin V G, Osetrov O I, Penionzhkevich Y E, Pyatkov Y V & Tiourin G P, *Phys Rev C*, 58 (1998) 1587.
39 Goyal S, Mandal S, Jhingan A, Sugathan P, Pal S, Behera B R, Golda K S, Singh H, Kalkal S, Singh V, Garg R, Siwal D, Kaur M, Saxena M, Kumar S, Verma S, Gupta M, Roy S & Singh R, *EPJ Web of Conf*, 86 (2015) 00013.
40 Shareef M, Prasad E, Jhingan A, Saneesh N, Golda K S, Vinodkumar A M, Kumar M, Shamlath A, Laveen P V, Visakh A C, Hosamani M M, Duggi S K, Devi P S, Jyothi G N, Tejaswi A, Patil P N, Sadhukhan J, Sugathan P, Chatterjee A & Pal S, *Phys Rev C*, 99 (2019) 024618.
41 Hinde D J, Ogata H, Tanaka M, Shimoda T, Takahashi N, A Shinohara, Wakamatsu S, Katori K & Okamura H, *Phys Rev C*, 39 (1989) 2268.
42 Kumar N, Verma S, Mohsina S, Sadhukhan J, Devi K R, Banerjee A, Saneesh N, Kumar M, Mahajan R, Thakur M, Kaur G, Rani A, Neelam, Yadav A, Kavita, Kumar R, Unnati, Mandal S, Kumar S, Behera B R, Golda K S, Jhingan A & Sugathan P, *Phys Lett B*, 814 (2021) 136062.
43 Kramers H A, *Phys (Amsterdam)*, 7 (1940) 284.